
# Conduction mechanism in polymeric membranes based on PEO or PVdF-HFP and containing a piperidinium ionic liquid

Electrochimica Acta 299 (2019) 979–986

Contents lists available at ScienceDirect

Electrochimica Acta

journal homepage: www.elsevier.com/locate/electacta

# Conduction mechanism in polymeric membranes based on PEO or PVdF-HFP and containing a piperidinium ionic liquid

Khalid Elamin [a, b, *], Mansoureh Shojaatalhosseini [b], Olesia Danyliv [a], Anna Martinelli [a], Jan Swenson [b]

[a] Department of Chemistry and Chemical Engineering, Chalmers University of Technology, SE-412 96 Gothenburg, Sweden
[b] Department of Physics, Chalmers University of Technology, SE-412 96 Gothenburg, Sweden

ARTICLE INFO

*Article history:*
Received 5 November 2018
Received in revised form
21 December 2018
Accepted 27 December 2018
Available online 4 January 2019

*Keywords:*
Poly(ethylene oxide)
Poly(vinylidene difluoride-co-hexafluoropropylene)
Ionic liquid and ionic conductivity

ABSTRACT

Two types of polymer electrolyte membranes were prepared using poly(ethylene oxide) (PEO) and poly(vinylidene difluoride-co-hexafluoropropylene) (PVdF-HFP), with different amounts of the ionic liquid N-methyl-N-propylpiperidinium bis(trifluoromethane-sulfonyl)imide ($[PP_{13}][TFSI]$) added. The results from differential scanning calorimetry and conductivity measurements show that in the case of PVdF-HFP membranes the glass transition temperature $T_g$ decreases and the room temperature ionic conductivity increases with increasing content of the ionic liquid (up to 60 wt.%). However, in the case of PEO based membranes $T_g$ is less significantly affected and the room temperature ionic conductivity increases only up to 30 wt.% of ionic liquid, beyond which a steady value of about $5 \cdot 10^{-5}$ S/cm is reached. The results from Raman spectroscopy show that the characteristic vibrational mode of the TFSI anion at ~742 $cm^{-1}$ is weakly affected in the membranes prepared from PVdF-HFP, whereas for those based on PEO it has a clearer composition dependence. These results suggest ion-ion and ion-polymer interactions of different nature, which together with the different nanomorphologies adopted by PEO and PVdF-HFP, as revealed by X-ray scattering, give rise to different composition dependences of the macroscopically measured ionic conductivity.



## 1. Introduction

During the last three decades, Solid Polymer Electrolytes (SPEs) have been extensively studied for development of energy storage and energy conversion devices [1–5], due to their compatibility for applications such as batteries, fuel cells, supercapacitors and sensors. SPEs possess many advantages over liquid electrolytes such as devoid of leakage, chemical and mechanical stabilities over a wide temperature range, non-volatility and limited dendrite formation. SPEs are easily prepared with various host solid matrix polymers such as poly(ethylene oxide) (PEO) [6], poly(vinylidene fluoride-co-hexafluoropropylene) (PVdF-HFP) [7], poly(acrylonitrile) (PAN) [8], poly(methyl methacrylate) (PMMA) [9], poly(vinyl chloride) (PVC) [10] and poly(vinyl pyrrolidone) (PVP) [11]. Among them, PEO is the most extensively studied, mainly due to the ability of dissolving alkali metal salts, its nontoxicity, a low glass transition temperature, the flexible backbone and the ease to form self-standing films. On the other hand, the polymer PVdF-HFP is an excellent candidate for SPEs with respect to processability, safety and chemical and mechanical stability over a wider temperature range.

At ambient conditions, most polymer electrolytes exhibit a very low ionic conductivity due to the presence of both amorphous and crystalline domains, the latter being detrimental for a high ionic mobility [12,13]. In fact, ionic dynamics are promoted in the amorphous domains where transport properties such as ionic conductivity, mechanical relaxations, diffusion, spin relaxation, *etc* are directly associated to the viscosity and glass transition related segmental motions of the polymer. To counteract the negative contribution of the crystalline domains, various approaches have been explored. One considers adding nanosized filler particles (e.g. $Al_2O_3$, $SiO_2$, $BaTiO_3$, $CeO_2$, *etc*), which may also improve the physicochemical properties of the membrane and create additional pathways for the mobile ions [14–19]. Another approach concerns the addition of low molecular weight co-solvents that act as plasticizer [1] reducing the degree of crystallinity and increasing the

* Corresponding author. Department of Chemistry and Chemical Engineering, Chalmers University of Technology, SE-412 96 Gothenburg, Sweden.
*E-mail addresses:* khalid.elamin@chalmers.se, khalid.elamin@gu.se (K. Elamin).

https://doi.org/10.1016/j.electacta.2018.12.154

flexibility of the polymer chains, thus lowering the glass transition temperature ($T_g$) with the result of an enhanced ionic conductivity [20]. A more recent and promising approach is to incorporate a room temperature ionic liquid (IL) into the polymeric matrix [21–23]. This brings new advantages, since ILs display high ionic conductivity even at room temperature, are inflammable, have a negligible vapor pressure and a wide range of thermal, chemical and electrochemical stabilities. These beneficial properties are thus transferred to the SPE [22–24].

Despite the high number of studies previously focused on polymer-IL-salt systems with and without the addition of nanoparticles or plasticizers, studies on neat polymer-IL membranes that explore wide concentration ranges have so far been sparse [25,26]. As a consequence, details on the direct polymer-IL interactions and the way these affect the conduction mechanism remain only partially explained. This work has the aim to provide new molecular level insights on this issue, with particular attention to the ionic mobility and degree of ionic association. Two types of polymer electrolyte membranes are investigated and directly compared, using PEO or PVdF-HFP as the polymer matrix and the ionic liquid N-methyl-N-propylpiperidinium bis(trifluoromethanesulfonyl)imide, [$PP_{13}$][TFSI], as the charge carrier, and covering the full compositional range. This ionic liquid has been chosen due to its suitable physical and chemical properties, such as high room temperature ionic conductivity ($1.5 \cdot 10^{-3}$ S cm$^{-1}$), low viscosity (117 mPa s) and wide window of electrochemical stability (from −3.3 to +2.3 V). This potential window is one of the widest among ILs [27]. The polymer electrolyte membranes were prepared by the solution cast method and characterized by DSC, X-ray scattering, impedance spectroscopy and Raman spectroscopy. Our results show that PEO based membranes perform better at low IL contents, whereas for IL contents above 50 wt. % PVdF-HFP based membranes provide higher ionic conductivities. We conclude that this behavior results from the concomitant phenomena of ionic dissociation, plasticizing effect and nanoscale morphology that in turn depend differently on composition in PEO and PVdF-HFP based membranes.

## 2. Experimental details

### 2.1. Membrane preparation

Two types of membranes were prepared based on poly(ethylene oxide) (PEO, molecular weight $5 \cdot 10^6$ g/mol, from Polysciences Inc.) or poly(vinylidene fluoride-co-hexafluoropropylene) (PVdF-co-HFP, molecular weight $4 \cdot 10^5$ g/mol, from Sigma Aldrich) with variable amounts of the ionic liquid N-methyl-N-propylpiperidinium bis(trifluoromethanesulfonyl)imide ([$PP_{13}$][TFSI], molecular weight 422.4 g/mol, from Solvionic). First, small quantities of polymer were added to an intermediate casting solvent (acetonitrile for PEO at room temperature and acetone heated at 313 K for PVdF-HFP) during magnetic stirring to avoid agglomeration. When the desired amount of the polymer had been added, the solution was stirred for an additional day in the case of PEO and two hours in the case of PVdF-HFP, before the ionic liquid [$PP_{13}$][TFSI] was added to the solution. This solution was stirred for 24 h to become homogenous, before being poured over a PTFE petri dish and dried at 323 K for 24 h to fully remove the solvent and possibly absorbed moisture. The complete removal of the solvent was verified by thermogravimetric analyses (TGA), performed on a TG 209 F1 Iris instrument from Netsch. This procedure resulted in free-standing thin solid polymer electrolyte films with a thickness of 100–150 μm. Films with an IL content above 60 wt.% showed poor mechanical properties and were not characterized further. For the molecular details of the used compounds we refer to Fig. 1.

### 2.2. Calorimetric measurements

Differential Scanning Calorimetry (DSC) measurements were carried out on pieces of 10–20 mg, encapsulated in a hermetic aluminium pan, using a TA Q1000 DSC instrument. The scanning procedure for each sample included a first cooling to 123 K with a cooling rate of 30 K/min followed by heating to 423 K at a rate of 10 K/min, under nitrogen atmosphere. This procedure was repeated three times. The glass transition temperature ($T_g$) and the melting of either the polymer phase or the IL ($T_m$) were analysed in the heating scan of the second cycle. During the different cycles the values of $T_g$, $T_c$, and $T_m$ were consistently observed at the same temperature.

### 2.3. Dielectric spectroscopy

Dielectric measurements were performed on a Novocontrol GmBH broadband dielectric spectrometer covering the frequency and temperature ranges $10^{-2} - 10^7$ Hz and 135 K–365 K, respectively. The value of the ionic conductivity has been taken from the plateau region of the real part of each ionic conductivity spectrum. The temperature was increased in steps of 5 K and at each temperature an equilibration time of 10 min was used. The polymer electrolyte membranes were placed between two gold plated electrodes with a diameter of 20 mm.

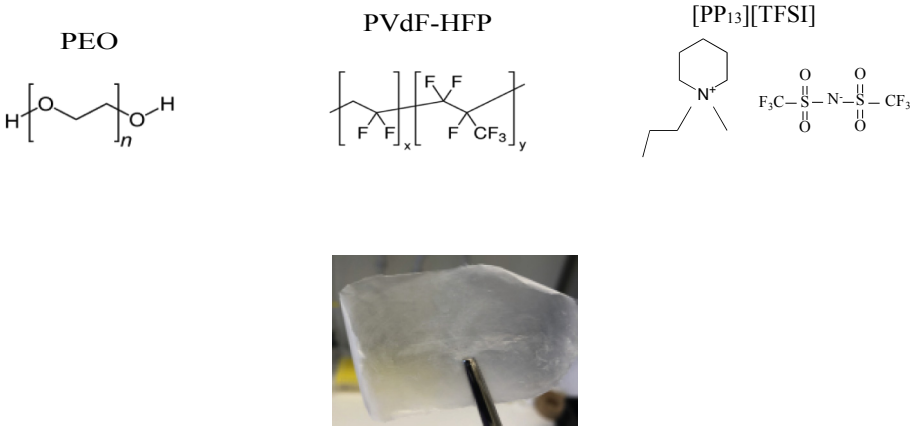


**Fig. 1.** Molecular structure of PEO, PVdF-HFP, and [$PP_{13}$][TFSI]. A picture of one PEO/IL membrane is also shown.

### 2.4. Vibrational spectroscopy

Raman spectra were collected with an InVia Reflex Renishaw spectrometer, using a 785 nm laser as the excitation source and a power at the sample limited to 3 mW to avoid local overheating. The spectra were obtained from 20 scans with 10 s of exposure covering the wavenumber range 100–4000 $cm^{-1}$. Where relevant, a peak-fit procedure based on Voigt type functions was implemented.

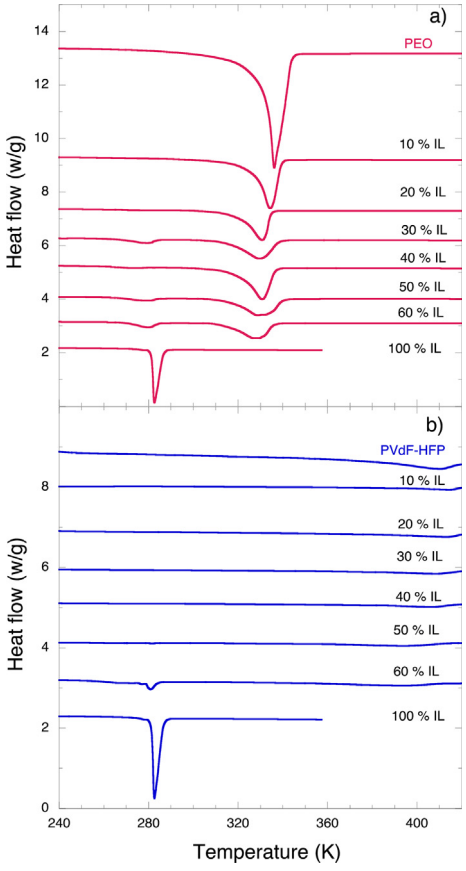


**Fig. 2.** DSC heating scans for the pure polymers PEO and PVdF-HFP, and the membranes based on PEO (a) and PVdF-HFP (b).

### 2.5. X-ray scattering

Small Angle X-ray Scattering measurements were performed on a Mat:Nordic instrument from SAXSLAB/Xenocs. The X-ray beam was produced by a Cu-radiation source and focused with a Micro-Max 003 X-ray generator from Rigaku. Pilatus 300K from Dectris was used as a detector of the scattered light. Pieces of the membranes were inserted at ambient conditions in-between two mica windows of a sandwich holder. By changing the distance between sample and detector, the transmission scattering in the scattering vector $q$ range 0.003–2.2 $Å^{-1}$ was collected. Sizes of different scattering objects were estimated from an observed structural correlation length $d$, where $d = 2\pi/q_{max}$ and $q_{max}$ is the position of the scattering peak. The collected spectra were analysed using the software WIRE 5.0 provided by Renishaw.

## 3. Results and discussion

### 3.1. Phase behavior

Fig. 2 shows the DSC curves of the pure polymers PEO and PVdf-HFP, as well as of the polymer electrolyte membranes as a function of the $[PP_{13}][TFSI]$ concentration. For both type of membranes two endothermic peaks are observed. The one at lower temperatures is attributed to the melting of $[PP_{13}][TFSI]$ and appears in a wider range of ionic liquid concentrations in PEO based membranes (above 30 wt.%) as compared to those based on PVdF-HFP (only above 50 wt.%), see also Table 1. This indicates that the ability of the ionic liquid to crystallize is more effectively suppressed in PVdF-HFP [28]. Nevertheless, the temperature for this melting is only slightly dependent on composition and is very similar for the two types of membranes. The other endothermic peak observed at higher temperatures is attributed to the melting of the polymer, PEO at 343 K and PVdF-HFP at 419 K. This peak is narrower and more pronounced for PEO based membranes, but its temperature decreases with increasing IL content for both polymers, see Fig. 3 and Table 1. It is worth noting that despite some previous works on polymer electrolytes have reported a merged peak including the melting of the ionic liquid and the polymer [29], in this current work we observe two distinct phase transitions with a separation of at least 30 K.

**Table 1**
Conductivity values measured at 300 K (σ, from dielectric spectroscopy) and phase transition temperatures ($T_g$ and $T_m$, from DSC) for different membranes prepared with PEO or PVdF-HFP. The activation energy, $E_a$, extracted from the Arrhenius plot of conductivity, as well as the structural parameters D (crystallites' size) and A (size of amorphous domains) are also included in the Table.

| | wt.% IL | $\sigma$ (S $cm^{-1}$) | $T_g$ (K) | $T_m^{IL}$ (K) | $T_m^{pol}$ (K) | $E_a$ (eV) | D (nm) | A (nm) |
|---|---|---|---|---|---|---|---|---|
| PEO | 0 | $9.0 \times 10^{-9}$ | 216 | – | 343 | – | 20 | 43 |
| | 10 | $3.3 \times 10^{-7}$ | 214 | – | 336 | – | 17 | 45 |
| | 20 | $8.5 \times 10^{-6}$ | 210 | – | 331 | – | | |
| | 30 | $3.4 \times 10^{-5}$ | 210 | 279 | 330 | – | 16 | 50 |
| | 40 | $9.6 \times 10^{-5}$ | 207 | 273 | 330 | – | | |
| | 50 | $6.0 \times 10^{-5}$ | 211 | 279 | 329 | – | | |
| | 60 | $7.0 \times 10^{-5}$ | 209 | 279 | 328 | – | 16 | 70 |
| PVdF-HFP | 0 | $9.7 \times 10^{-11}$ | 236 | – | 419 | 0.57 | 15 | 8 |
| | 10 | $5.4 \times 10^{-8}$ | 233 | – | 414 | 0.39 | | 9 |
| | 20 | $5.2 \times 10^{-7}$ | 232 | – | 413 | 0.34 | | |
| | 30 | $9.3 \times 10^{-6}$ | 223 | – | 408 | 0.29 | 9 | 12 |
| | 40 | $2.4 \times 10^{-5}$ | 214 | – | 407 | 0.27 | | |
| | 50 | $8.0 \times 10^{-5}$ | 211 | 281 | 395 | 0.26 | | |
| | 60 | $3.6 \times 10^{-4}$ | 207 | 281 | 393 | 0.22 | 8 | 13 |
| $[PP_{13}][TFSI]$ | 100 | $1.6 \times 10^{-3}$ | 240 | 283 | – | 0.18 | – | – |

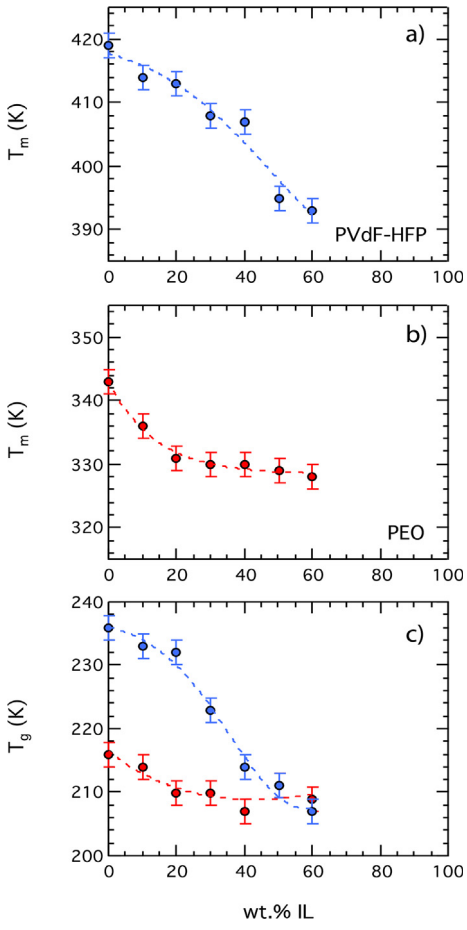


**Fig. 3.** Melting temperature ($T_m$) and glass transition temperature ($T_g$) of the polymer as a function of IL content in membranes prepared with PEO (red symbols) or PVdF-HFP (blue symbols).

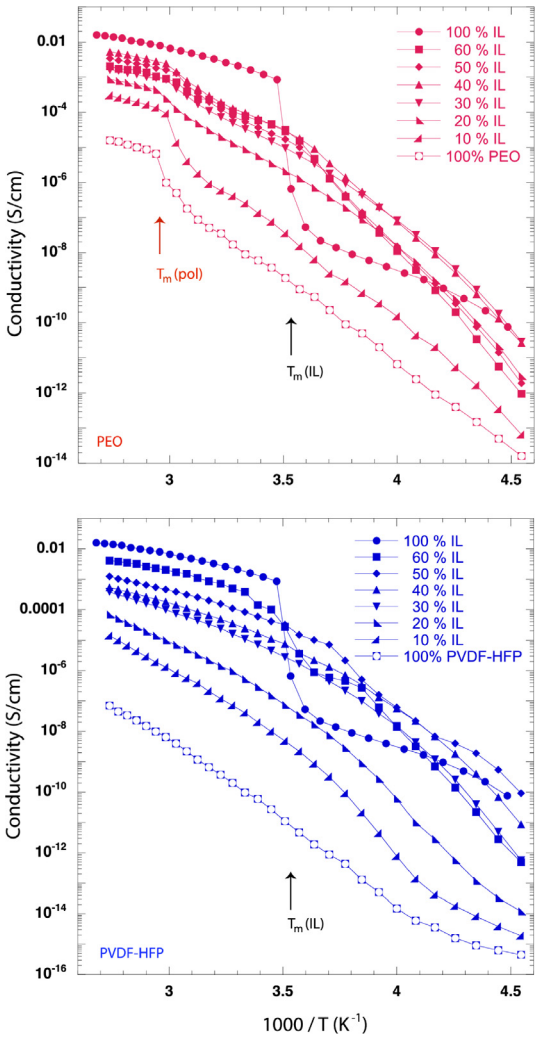


**Fig. 4.** Arrhenius plots of the ionic conductivity for membranes based on PEO (top) and on PVdF-HFP (bottom). Vertical lines indicate temperatures associated to phase changes.

We also observe that the change of $T_m$ is more pronounced in PVdF-HFP membranes (Fig. 3a) than in PEO (Fig. 3b) and that the rate of this change is different in the two polymers. The glass transition temperature ($T_g$) also changes more significantly in PVdF-HFP membranes (Fig. 3c), indicative of a clearer plasticizing effect of the IL in this polymer. Most notable is that for membranes containing more than 40 wt.% of the IL, the $T_g$ of PEO and PVdF-HFP become comparable.

### 3.2. Ionic conductivity

Fig. 4 shows an Arrhenius plot of the ionic conductivity for both polymer electrolyte membranes (PEO in panel a, and PVdF-HFP in panel b). The ionic conductivity of neat [$PP_{13}$][TFSI] shows a jump upon heating at 1000/T ≈ 3.5, which is attributed to the solid-liquid transition observed at 283 K in the DSC trace. Conductivity values measured in the liquid phase are in perfect agreement with those reported by Stepnjak et al. for an equivalent IL [30]. In PEO based membranes, a raise in conductivity is observed at this same temperature followed by an increase at about 340 K, which according to the DSC results is attributed to the melting of the crystalline regions of the polymer. The relative vicinity of these two phase-transitions makes it difficult to extract more precise information on e.g. the activation energy of ionic conduction, $E_a$, in the membranes, although a qualitative observation is that at temperatures higher than 340 K the dependence of conductivity on inverse temperature is very little dependent on composition. A similar behavior has been reported in previous studies of PEO-ionic liquid and PEO-salt systems [17,29,31–36].

By comparison, membranes based on PVdF-HFP show a discontinuous increase of conductivity at only one temperature, corresponding to the melting of the ionic liquid, but only for membranes with 50 wt.% and 60 wt.% of IL. This agrees with the DSC results that show phase transitions only for these compositions (see Fig. 2b). The melting temperature of PVdF-HFP falls outside the temperature window investigated and shown in Fig. 4, which explains why no further conductivity discontinuities are observed. The smooth and almost Arrhenius temperature dependent behavior of all membranes based on PVdF-HFP above 283 K (1000/T = 3.5) allows estimating an approximative value of the activation energy $E_a$. The use of the Arrhenius law is justified by the relatively narrow temperature range investigated. Values of $E_a$ are reported in Table 1 and show a smooth and monotonic decrease with the amount of IL added, indicating that the conduction mechanism depends on composition. We observe that the value of $E_a$ equal to 0.18 eV found for the pure IL is comparable to that recently reported by Ferrari et al. [37] for N-methoxyethyl-N-methylpyrrolidinium bis(trifluoromethanesulfonyl)imide.

The specific effect of the polymer on the ionic conductivity is visualized in Fig. 5, which compares the performance of

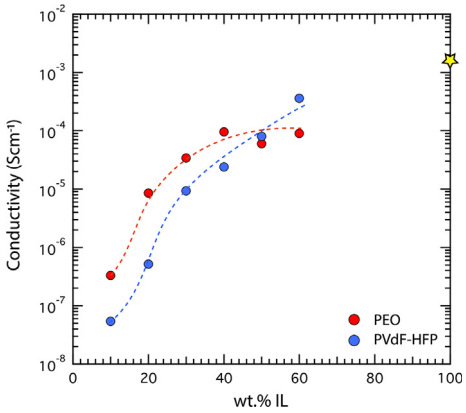


**Fig. 5.** Composition dependence of the ionic conductivity measured at 300 K for membranes based on PEO (red) and PVdF-HFP (blue). The value measured for the neat IL is also shown as a yellow star.

membranes based on PEO or PVdF-HFP at room temperature (*i.e.* at 300 K). PEO based membranes show a superior behavior for low IL contents (*i.e.* below 50 wt.%) with conductivity values up to about one order of magnitude higher than PVdF-HFP based membranes. One reason for this difference can be found in the glass transition temperature of the two polymers, which is consistently lower in PEO based membranes (see Fig. 3c). Thus, at comparable compositions and at room temperature the segmental motion of the backbone in PEO is likely to be faster and therefore more favorable for a high ionic mobility. Similarly, the higher ionic conductivity observed in PVdF-HFP based membranes for IL contents above 50 wt.% can be rationalized by the significantly lowered $T_g$ values. It is intriguing though that PEO based membranes show no significant increase in conductivity in the range 40–60 wt.% of IL, as opposed to the case of PVdF-HFP membranes that show a monotonic increase. A similar trend has been observed in polymer electrolyte membranes based on PEO and the magnesium triflate salt ([Mg][$Tf_2$]) containing variable amounts of the IL 1-ethyl-3 methylimidazolium trifluoromethanesulfonate ([EMI][Tf]) [35]. In that work, the decrease in room temperature ionic conductivity observed for [EMI][Tf] contents above 50 wt.% was assigned to the negative effect of ionic association.

### 3.3. Competing intermolecular interactions

The nature of ion-ion and ion-polymer interactions established in the investigated membranes has been studied by Raman spectroscopy in the spectral range 720–760 $cm^{-1}$ where the expansion-contraction mode of the TFSI anion is found, Fig. 6a and 6b. The frequency of this mode correlates with the strength of interaction between $TFSI^-$ and its chemical environment [38], with blue frequency shifts indicating more strongly bound anions. Our spectral analysis reveals a red shift with increasing PEO content, which we assign to the affinity of the negatively charged oxygen groups in PEO with the cations, as previously also proposed for other PEO-IL or PEO-salt systems [39,40]. This affinity competes with the native cation-anion interactions and leaves the TFSI anions less strongly bound than in the case of the neat IL. It is interesting to mention that this same behavior has recently been observed also in membranes prepared from PVdF-HFP and the IL [EMIM][TFSI] upon addition of low molecular weight poly(ethylene) glycol (PEG) [41]. Most relevant is that the composition below which the red shift becomes significant is 50 wt.% of IL, which is equivalent to approximately 10 oxygen atoms per cation-anion pair. This value thus represents the number of oxygens needed to form the PEO-

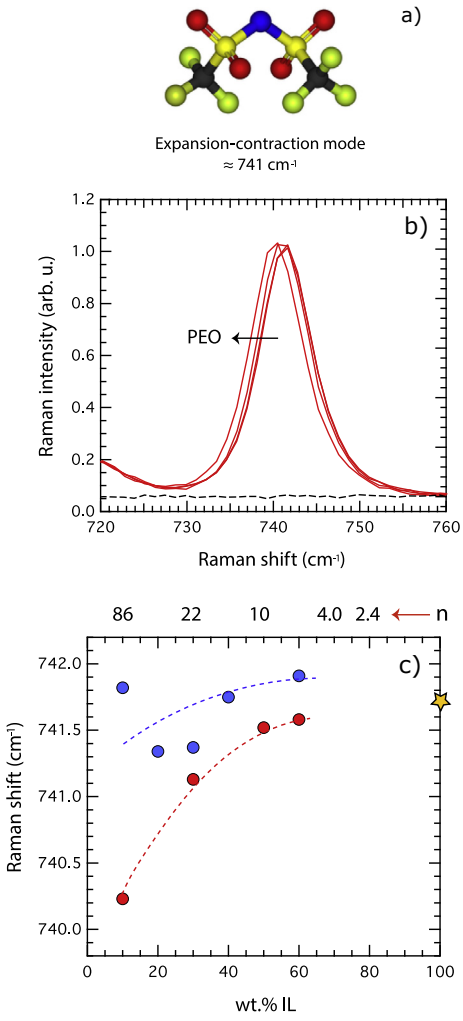


**Fig. 6.** Molecular structure of the TFSI anion and the expected frequency of its expansion-contraction mode (a). Raman spectra of PEO based membranes in the frequency range of the expansion-contraction mode (b). The black dashed line indicates the negligible contribution of PEO in the analysed spectral window. Composition dependence of the Raman shift found in PEO (red) and PVdF-HFP (blue) based membranes (c). The value measured for the neat IL is shown as a yellow star. On the top axis the number of oxygen atoms available per cation-anion pair, *n*, is also shown.

cation complex able to liberate the TFSI anion, and is in very good agreement with the value found by Kösters et al. in the investigation of PEO-[EMIM][I] mixtures [25]. This can be compared to the known value of 4 or 5 oxygen atoms needed to form a $Li^+$-PEO complex [40], the $Li^+$ being a much smaller and charge dense cation than [$PP_{13}^+$] or [$EMIM^+$].

In the case of PVdF-HFP membranes, the frequency shift with composition is much less pronounced, while the systematically higher wavenumbers suggest an overall higher degree of cation-anion association than for the case of PEO. A schematic illustration of the different types of [$PP_{13}$][TFSI]–polymer interactions established is proposed in Fig. 7.

### 3.4. Nanoscale morphology

Further insights on the mechanism of ionic conduction can be retrieved from the local structure of the polymer phase, which we have investigated by X-ray scattering methods in the wide and small angle scattering modes. Interesting features are observed in the higher q range 0.5–2.2 $Å^{-1}$ (WAXS) and in the lower q range

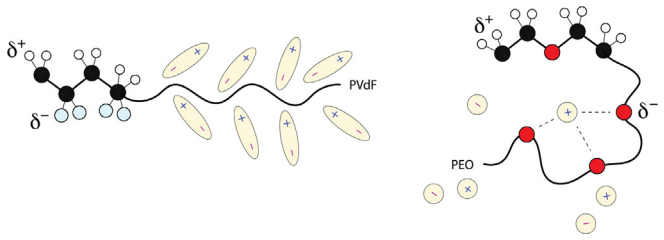


**Fig. 7.** Schematic illustration of the polymer-ion interactions established in PVdF-HFP (left) and PEO (right) based membranes, the latter being able to promote cation-anion dissociation through favorable $O^-$ – cation interactions. The atoms are coloured as follows: red (O), blue (F), white (H) and black (C).

0.003–0.300 $Å^{-1}$ (SAXS-ESAXS), as shown in Figs. 8 and 9, respectively. In the higher q range, features related to the crystalline phases in the polymer are observed. However, the amorphous halo and peaks attributed to the IL itself also contribute in this q interval.

Pure PEO is known to have a high degree of crystallinity, between 70 and 80% [29,42], and the observed peaks in the range 1.3–1.8 $Å^{-1}$ (Fig. 8, top) are assigned to inter-chain distances of 3.2–4.6 Å within the crystalline domains [43]. Upon addition of the IL these scattering peaks shift slightly towards lower q values, in agreement with the results of Chaurasia et al. [29]. By use of the Debye-Scherrer's equation,[1] we have estimated the crystallites' size, D, to depend weakly on composition, changing from ~20 nm in pure PEO to ~16 nm in all PEO-IL membranes, see also Table 1. The analysis of the WAXS data shown in the bottom panel of Fig. 8 [44–46] reveals that pure PVdF-HFP has a degree of crystallinity of ~29%,[2] in agreement with the results presented by Abbrent et al. [44]. Upon addition of the IL, PVdF-HFP changes from the α-to the γ-phase [44,46,47], while the degree of crystallinity is estimated to be ~20%, similarly to what has previously been found in a PVdF-HFP/[Li][TFSI] based system [44]. Moreover, the crystallites' size changes from ~15 nm in pure PVdF-HFP to ~9 nm in the PVdF-HFP-IL membranes, as also reported in Table 1. These results indicate that the effect of the IL on the crystalline phase of the polymer is stronger in PVdF-HFP than in PEO, which is consistent with the conclusions already drawn from the DSC results. DSC and X-Ray data also agree in showing that the crystallinity of the polymer is slightly lower in the membranes than in the pure polymer, but varies very weakly with composition.

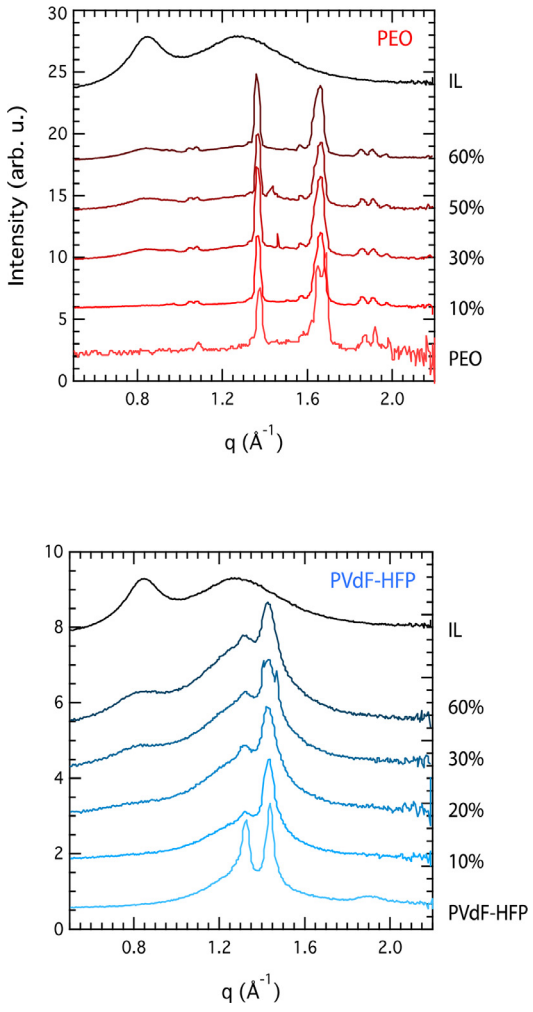


**Fig. 8.** WAXS data recorded for selected membranes based on PEO (top) or PVDF-HFP (bottom) with different weight fraction of the IL.

In the lower q range of the X-ray scattering profile, Fig. 9, a feature often referred to as the matrix knee is seen, which has been previously assigned to the distance between the crystallites [48] or, in other words, to the size of the amorphous domains in e.g. Nafion type of membranes. The amorphous domains, A, are estimated to be ~43 and ~8 nm large in pure PEO and PVdF-HFP, respectively (see also Table 1). For both polymers, the matrix knee feature shifts to lower q values, confirming that the IL accommodates preferentially in the amorphous domains (for an IL content of 60 wt.% the amorphous domains have an estimated size of 70 and 13 nm in PEO and PVdF-HFP respectively). However, in PEO based membranes the matrix knee is less defined and also shows a second higher-q contribution attributable to the existence of more than one type of crystalline phase. The morphological information that we have achieved reveal larger correlation lengths in PEO than in PVdF-HFP membranes, but also a larger expansion of the amorphous domains in PEO as a result of added IL. For high IL contents, this may reflect a structural loss due to excessive swelling, possibly similar to the transition into a polymer-in-ionic liquid system as recently proposed by Kösters et al. [25].

To summarize, we have presented a comparative investigation of PEO and PVdF-HFP based polymer electrolytes containing variable amounts of the IL [$PP_{13}$][TFSI]. Our results reveal that the superior ionic conductivity of PEO based membranes at low IL content (i.e. below 50 wt.%) is due to a favourably low $T_g$ (DSC) coupled to a certain degree of ionic dissociation (Raman). The presence of IL, however, influences the properties of PVdF-HFP more markedly, which results in a significantly reduced $T_g$ for this polymer that in fact becomes comparable and even lower than the one found for PEO (DSC). For IL contents above 50 wt.% the ionic conductivity of PVdF-HFP membranes is higher, which is explained by the loss of the favorable properties of IL-PEO mixtures discussed above, and the more pronounced plasticizing effect of [$PP_{13}$][TFSI] on PVdF-HFP. For both polymers, the degree of crystallinity changes moderately with the amount of IL (X-ray scattering), in agreement with the results found for PEO-[EMIM][Tf] mixtures [35]. However, from the position of the characteristic X-ray peaks in the low and the high q range, we can conclude that the structural inhomogeneities in PEO membranes occur over a larger length scale

[1] $D = (0.94 \cdot \lambda)/(FWHM \cdot \cos(\theta))$, where D is the estimated size of the crystallites, 0.94 is a factor that can vary between 0.5 and 1, λ is the wavelength of the incoming X-ray source, and θ is the scattering angle. The equation used in this form assumes crystallites of spherical shape and is an approximation since the FWHM contains contribution from the materials but also from the instrumental resolution.

[2] An estimation that does not take into account the different densities of amorphous and crystalline PVdF, which however differ from each other by only 10%.

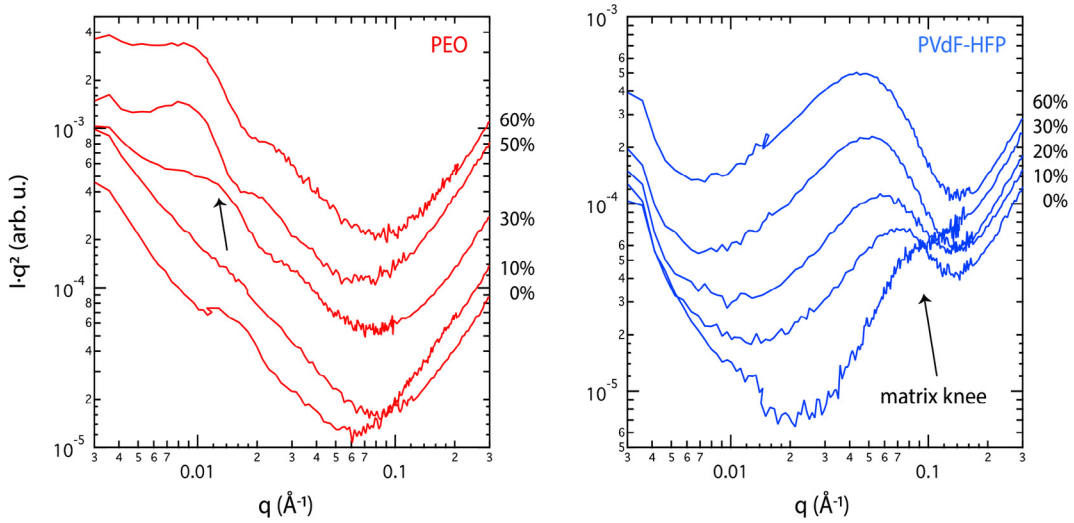


**Fig. 9.** SAXS data recorded for selected membranes based on PEO (left) and on PVDF-HFP (right) with different weight fraction of the IL.

(larger crystallites and wider amorphous domains) than in PVdF-HFP, and thus explain the more evident melting transitions observed with DSC. In fact, the combined information from the DSC and X-ray data indicates different morphologies in the two types of polymers, with mainly spatial confinement in PVdF-HFP based membranes and more pronounced IL-polymer interactions over wider domains in those based on PEO.

## 4. Conclusions

This study demonstrates that transport and structural properties in PEO and PVdF-HFP based membranes depend differently on the amount of added ionic liquid. In practice, PEO based membranes perform better at ionic liquid contents lower than 50 wt.%, while PVdF-HFP based membranes are superior above this threshold. We demonstrate that competing factors lay behind this behavior, such as the strength of ion-ion association, the nature of ion-polymer interaction, and the availability of amorphous domains.

In PVdF-HFP, ions are not strongly associated to the polymer, and behave locally as in the pure IL. Therefore, the conductivity increases continuously with the concentration of the IL due to conduction pathways that increase in both number and size. In PEO, and at low IL concentrations, the cations are strongly associated to the ether oxygens and the conduction mechanism is more similar to that found in ordinary polymer electrolytes (e.g. with a Li-salt). However, at about 40 wt.% of IL or above there are not enough ether oxygens for all the cations and the population of anion-associated cations increases. At these conditions, the conductivity mechanism is more similar to that of bulk IL and in PVDF-HFP, but there are less cations participating in this mechanism and larger restrictions of pathways due to a larger degree of crystallization. In the crossover from a conductivity mechanism assisted by the polymer segmental motion to a 'ordinary' IL conductivity, the conductivity may even decrease (as we see when going from 40 to 50 wt.% of IL) due to a dilution of the polymer network.

These results, that discriminate the individual roles of PEO and PVdF-HFP, can serve as a guideline in the design of mixed PVdF-HFP/PEO polymer electrolytes, although predicting the optimal blend composition remains a challenge. In fact, whether the mixed membrane should be PEO or PVdF-HFP rich is a matter of future investigation since the answer depends on how the IL will distribute between the two polymer phases.

## Acknowledgements

The authors wish to acknowledge the Swedish Energy Agency (grant no 42894-1), the Knut & Alice Wallenberg Foundation (Wallenberg Academy Fellows, Grant no 2016-0220) and the Swedish Foundation for Strategic Research (SSF, grant no FFL 15 - 0092) for financial support.

## References

[1] J.R. MacCallum, C.A. Vincent (Eds.), Polymer Electrolyte Reviews, vols. 1 and 2, Elsevier Applied Science, London, 1987, p. 1989.
[2] F.M. Gray, Solid Polymer Electrolytes: Fundamental and Technological Applications, VCH Publishers, New York, 1991.
[3] B. Scrosati (Ed.), Applications of Electroactive Polymers, Chapman and Hall, London, 1993.
[4] F.M. Gray, Polymer Electrolytes, Royal Society of Chemistry, Cambridge, 1997.
[5] R.C. Agrawal, G.P. Pandey, Solid polymer electrolytes: materials designing and all-solid-state battery applications: an overview, J. Phys. Appl. Phys. 41 (2008) 223001–223019.
[6] M. Shojaatalhosseini, K. Elamin, J. Swenson, Conductivity-relaxation relations in nanocomposite polymer electrolytes containing ionic liquid, J. Phys. Chem. B 121 (2017) 9699–9707.
[7] A. Martinelli, A. Fernicola, S. Panero, A. Matic, H. Ohno, P. Jacobsson, B. Scrosati, L. Börjesson, Physical properties of proton conducting membranes based on a protic ionic liquid, J. Phys. Chem. B 111 (2007) 12462–12467.
[8] F. Croce, F. Gerace, G. Dautzenberg, S. Passerini, G.B. Appetecchi, B. Scrosati, Synthesis and characterization of highly conducting gel electrolytes, Electrochim. Acta 39 (1994) 2187–2194.
[9] O. Bohnke, G. Frand, M. Rezrazi, C. Rousselot, C. Truche, Fast ion transport in new lithium electrolytes gelled with PMMA. 1. Influence of polymer concentration, Solid State Ionics 66 (1993) 97–104.
[10] G. Pistoia, A. Antonini, G. Wang, Impedance study on the reactivity of gel polymer electrolytes towards a lithium electrode, J. Power Sources 58 (1996) 139–144.
[11] S. Passerini, J.M. Rosolen, B. Scrosati, Plasticized carbon electrodes of interest for lithium rocking chair batteries, J. Power Sources 45 (1993) 333–341.
[12] C. Berthier, W. Gorecki, M. Minier, M.B. Armand, J.M. Chabagno, P. Rigaud, Microscopic investigation of ionic conductivity in alkali metal salts-poly(ethylene oxide) adducts, Solid State Ionics 11 (1983) 91–95.
[13] E. Quartarone, P. Mustarelli, Electrolytes for solid-state lithium rechargeable batteries: recent advances and perspectives, Chem. Soc. Rev. 40 (2011) 2525–2540.
[14] F. Capuano, F. Croce, B. Scrosati, Composite polymer electrolytes, J. Electrochem. Soc. 138 (1991) 1918–1922.
[15] F. Croce, G.B. Appetecchi, L. Persi, B. Scrosati, Nanocomposite polymer electrolytes for lithium batteries, Lett. Nat. 394 (1998) 456–458.
[16] B. Kumar, L.G. Scanlon, R.J. Spry, On the origin of conductivity enhancement in polymer-ceramic composite electrolytes, J. Power Sources 96 (2001) 337–342.
[17] S.A. Hashmi, A.K. Thakur, H.M. Upadhyaya, Experimental studies on polyethylene oxide–NaClO4 based composite polymer electrolytes dispersed with Na2SiO3, Eur. Polym. J. 34 (1998) 1277–1282.

[18] G.P. Pandey, S.A. Hashmi, R.C. Agrawal, Hot-press synthesized polyethylene oxide based proton conducting nanocomposite polymer electrolyte dispersed with SiO2 nanoparticles, Solid State Ionics 179 (2008) 543–549.
[19] J. Zhou, P.S. Fedkiw, Ionic conductivity of composite electrolytes based on oligo (ethylene oxide) and fumed oxides, Solid State Ionics 166 (2004) 275–293.
[20] S. Rajendran, V.S. Bama, A study on the effect of various plasticizers in poly (vinyl acetate)-poly(methyl methacrylate) based gel electrolytes, J. Non-Cryst.Solids 356 (2010) 2764–2768.
[21] J.H. Shin, W.A. Henderson, S. Passerini, PEO-based polymer electrolytes with ionic liquids and their use in lithium metal-polymer electrolyte batteries, J. Electrochem. Soc. 152 (2005) A978–A983.
[22] J.W. Choi, G. Cheruvally, Y.H. Kim, J.K. Kim, J. Manuel, P. Raghavan, C.E. Song, Poly(Ethylene oxide)-based polymer electrolyte incorporating room-temperature ionic liquid for lithium batteries, Solid State Ionics 178 (2007) 1235–1241.
[23] Kh Ghandi, A review of ionic liquids, their limits and applications, Green Sustain. Chem. 4 (2014) 44–53.
[24] S.K. Chaurasia, R.K. Singh, S. Chandra, Effect of ionic liquid on the crystallization kinetics behaviour of polymer poly (ethylene oxide), CrystEngComm 15 (2013) 6022–6034.
[25] J. Kösters, M. Schönhoff, N.A. Stolwijk, Mass and charge transport in the polymer-Ionic-liquid system PEO–EMImI: from ionic-liquid-in-polymer to polymer-in-ionic- liquid electrolytes, J. Phys. Chem. B 119 (2015) 5693–5700.
[26] C. Tiyapiboonchaiya, D.R. MacFarlane, J. Sun, M. Forsyth, Polymer-in-Ionic-Liquid electrolytes, Macromol. Chem. Phys. 203 (2002) 1906–1911.
[27] M. Galinski, A. Lewandowski, I. Stepniak, Ionic liquids as electrolytes, Electrochim. Acta 51 (2006) 5567–5580.
[28] P. Prabakaran, R.P. Manimuthu, S. Gursamy, E. Sebasthiyan, Plasticized polymer electrolyte membranes based on PEO/PVdF-HFP for use as an effective electrolyte in lithium-ion batteries, Chin. J. Polym. Sci. 35 (2017) 407–421.
[29] S.K. Chaurasia, R.K. Singh, S. Chandra, Structural and transport studies on polymeric membranes of PEO containing ionic liquid, EMIM-TY: evidence of complexation, Solid State Ionics 183 (2011) 32–39.
[30] I. Stepniak, E. Andrzejewska, A. Dembna, M. Galinski, Characterization and application of N-methyl-N-propylpiperidinium bis(trifluoromethanesulfonyl) imide ionic liquid–based gel polymer electrolyte prepared in situ by photopolymerization method in lithium ion batteries, Electrochim. Acta 121 (2014) 27–33.
[31] B.K. Money, K. Hariharan, J. Swenson, Relation between structural and conductivity relaxation in PEO and PEO based electrolytes, Solid State Ionics 262 (2014) 785–789.
[32] G.P. Pandey, Y. Kumar, S.A. Hashmi, Ionic liquid incorporated PEO based polymer electrolyte for electrical double layer capacitors: a comparative study with lithium and magnesium systems, Solid State Ionics 190 (2011) 93–98.
[33] Y. Kumar, S.A. Hashmi, G.P. Pandey, Lithium ion transport and ion–polymer interaction in PEO based polymer electrolyte plasticized with ionic liquid, Solid State Ionics 201 (2011) 73–80.
[34] T.M.W.J. Bandara, M.A.K.L. Dissanayake, I. Albinsson, B.E. Mellander, Mobile charge Carrier concentration and mobility of a polymer electrolyte containing PEO and $Pr4N^{+}I^{-}$ using electrical and dielectric measurements, Solid State Ionics 189 (2011) 63–68.
[35] Y. Kumar, S.A. Hashmi, G.P. Pandey, Ionic liquid mediated magnesium ion conduction in poly (ethylene oxide) based polymer electrolyte, Electrochim. Acta 56 (2011) 3864–3873.
[36] J.S. Moreno, M. Armand, M.B. Berman, S.G. Greenbaum, B. Scrosati, S. Panero, Composite PEOn:NaTFSI polymer electrolyte: preparation, thermal and electrochemical characterization, J. Power Sources 248 (2014) 695–702.
[37] S. Ferrari, E. Quartarone, P. Mustarelli, A. Magistris, S. Protti, S. Lazzaroni, M. Fagnoni, A. Albini, A binary ionic liquid system composed of N-methoxyethyl-N-methylpyrrolidinium bis(trifluoromethanesulfonyl)-imide and lithium bis(trifluoromethanesulfonyl)imide: a new promising electrolyte for lithium batteries, J. Power Sources 194 (2009) 45–50.
[38] I. Rey, P. Johansson, J. Lindgren, J.C. Lassègues, J. Grondin, L. Servant, Spectroscopic and theoretical study of (CF2SO2)2N-(TFSI-) and $(CF_3SO_2)_2NH$ (HTFSI), J. Phys. Chem. A 102 (1998) 3249–3258.
[39] K. Hoher, P.F. Cardoso, L.F. Lepre, R.A. Ando, L.J.A. Siqueira, Molecular dynamics and a spectroscopic study of sulfur dioxide absorption by an ionic liquid and its mixtures with PEO, Phys. Chem. Chem. Phys. 18 (2016) 28901–28910.
[40] L.T. Costa, M.C.C. Ribero, Molecular dynamics simulation of polymer electrolytes based on poly (ethylene oxide) and ionic liquids. I. Structural properties, Chem. Phys. 124 (2006) 184902–184909.
[41] H. Zhao, C. Chen, R. Zhao, L. Feng, Exceptional point engineered glass slide for microscopic thermal mapping, Nat. Commun. 9 (2018) 1764–1771.
[42] A.M. Rocco, R.P. Pereira, M.I. Felisberti, Miscibility, crystallinity and morphological behavior of binary blends of poly(ethylene oxide) and poly(methyl vinyl ether-maleic acid), Polymer 42 (2001) 5199–5205.
[43] Y. Takahashi, H. Tadokoro, Structural studies of polyethers, (-(CH2)m-O-)n. X. Crystal structure of poly(ethylene oxide), Macromolecules 6 (1973) 672–675.
[44] S. Abbrent, J. Plestil, D. Hlavata, J. Lindgren, J. Tegenfeldt, Å. Wendsjö, Crystallinity and morphology of PVdF–HFP-based gel electrolytes, Polymer 42 (2001) 1407–1416.
[45] J. Buckley, P. Cebe, D. Cherdack, J. Crawford, B.S. Ince, M. Jenkins, J. Pan, M. Reveley, N. Washington, N. Wolchover, Nanocomposites of poly(vinylidene fluoride) with organically modified silicate, Polymer 47 (2006) 2411–2422.
[46] R. Hasegawa, Y. Takahashi, Y. Chatani, H. Tadokoro, Crystal structures of three crystalline forms of poly(vinylidene fluoride), Polym. J. 3 (1972) 600–610.
[47] T. Kallio, K. Jokela, H. Ericson, R. Serimaa, G. Sundholm, P. Jacobsson, F. Sundholm, Effects of a fuel cell test on the structure of irradiation grafted ion exchange membranes based on different fluoropolymers, J. Appl. Electrochem. 33 (2003) 505–514.
[48] H. Mendil-Jakani, I.Z. López, V.H. Mareau, L. Gonona, Optimization of hydrophilic/hydrophobic phase separation in sPEEK membranes by hydrothermal treatments, Phys. Chem. Chem. Phys. 19 (2017) 16013–16022.